Initiation and propagation of shear zones in a heterogeneous continental lithosphere

Andrea Tommasi, Alain Vauchez, Bertrand Daudré

JOURNAL OF GEOPHYSICAL RESEARCH, VOL. 100, NO. B11, PAGES 22,083–22,101, NOVEMBER 10, 1995

Initiation and propagation of shear zones in a heterogeneous continental lithosphere

Andréa Tommasi and Alain Vauchez

Laboratoire de Tectonophysique, CNRS/Université de Montpellier II, Montpellier, France

Bertrand Daudré

IREMIA, Université de la Réunion, St.Denis, La Réunion, France

Abstract. Continental plates represent rheologically heterogeneous media in which complex finite strain fields may develop due to interaction of plate tectonic processes with intraplate heterogeneities. Such a deformation pattern is displayed by the Borborema shear zone system in northeastern Brazil. It involves continental-scale, curvilinear, E-W trending right-lateral transcurrent shear zones that branch off from a major NE trending, right-lateral strike-slip deformation zone formed at the northern termination of the São Francisco craton and that finally terminate in transpressive metasedimentary belts. We suggest that this strain field results from the compressional deformation of a highly heterogeneous continental lithosphere composed of a stiff domain (craton) and rheologically weaker domains (basins). The effect of a low-viscosity domain on the deformation of a continental plate and, in particular, the perturbation induced by this domain on the development of a shear zone formed at the termination of a stiff block were investigated using numerical modeling. The low-strength domain induces an enhanced strain localization, and the geometry of the shear zone is significantly modified. It is either split, forming a branched shear zone system in which one branch maintains its original orientation while the other rotates toward the low-viscosity domain, or completely rotated toward the weak block. The perturbation of the finite strain field depends on the ability of the weak domain to accommodate deformation, which is controlled by its initial viscosity contrast relative to the surrounding lithosphere, its orientation relative to the convergence direction, and its distance from the shear zone initiated at the termination of the stiff block. The interaction between imposed boundary conditions (tectonic forces and plate geometry) and the internal structure of the plate may give rise to highly heterogeneous strain fields, as exhibited by the Borborema shear zone system, in which intraplate rheological heterogeneities induce the development of branched or sinuous shear zones. A heterogeneous continental plate subjected to a normal convergence may therefore display significant lateral variations in strain intensity, with shear zones bordering nearly undeformed blocks, and in deformation regimes and vertical strains that would result in contrasting metamorphic and uplift histories.

Introduction

Continents are built and modified through a long and complex history involving accretion of exotic terranes, formation of subduction zones at their margins, extensional tectonics, and continental collision. Their long geodynamic histories result in the coexistence of domains formed during distinct tectonomagmatic episodes and give rise to a mosaic-like structure. The continental lithosphere therefore cannot be regarded as a simple, mechanically homogeneous medium. Displacement fields developed within a deforming continent reflect both a first-order, large-scale kinematic pattern associated with active plate tectonic processes and a second-order, shorter-wavelength kinematic pattern associated with the geometry of plate boundaries and with intraplate heterogeneities [*Vauchez and Tommasi*, 1993].

Paper number 95JB02042.
0148-0227/95/95JB-02042$05.00

Irregular geometries of plate boundaries may locally influence the boundary conditions. Abrupt variations in boundary conditions generate complex stress/strain fields, frequently characterized by strain partitioning and localization in large-scale shear zones. This effect has been examined for the Himalayan collision, based on physical, analogue models [*Peltzer and Tapponnier*, 1988] and numerical models [*England and McKenzie*, 1982; *Vilotte et al.*, 1982, 1984, 1986; *England and Houseman*, 1985, 1986, 1989; *Houseman and England*, 1993].

The mosaic-like structure of continents induces lateral variations in lithospheric thicknesses, geothermal gradients, and tectonic fabrics that characterize both structural and thermal heterogeneities within continental plates. However, the influence of these intraplate heterogeneities on continental deformation fields has not been investigated extensively. Structural heterogeneities such as ancient lithospheric faults or suture zones between different terranes of a continental plate may lead to localized tectonic flow. These structures are generally characterized by lattice-preferred orientations of minerals and may thus display pronounced anisotropic mechanical properties [*Vauchez and Barruol*, 1995]. However, the limited experimental

data on anisotropic flow properties of geological materials still hinder evaluations of the effects of preexisting structures on subsequent deformations of the continental lithosphere.

Lateral variations in continental geotherms characterize intraplate thermal heterogeneities and give rise to rheological heterogeneities, since under lithospheric conditions, rock-forming minerals deform dominantly by dislocation creep, a mechanism that displays an exponential dependence on temperature. The strength of the continental lithosphere increases with decreasing geothermal gradients. Thus domains with lower geothermal gradients than the surrounding lithosphere represent stiff rheological heterogeneities, whereas domains with higher geothermal gradients are characterized by lower strengths than the surrounding lithosphere.

Most continental plates consist of an old cratonic nucleus surrounded by more recently accreted terranes. Cratonic blocks usually display a thicker lithosphere and a lower geothermal gradient and represent domains of high stiffness relative to the surrounding lithosphere. These stiff intraplate heterogeneities significantly affect the mechanical response of the continental lithosphere to tectonic forces. In the Canadian Cordillera, for example, *Lowe and Ranalli* [1993] correlate a change in deformation pattern with the strength contrast resulting from different lithospheric thicknesses and thermal regimes in the Cordillera and the North American craton. The perturbation of the first order strain field by a cold and stiff inclusion in a continental plate during a collisional orogeny has also been documented for the Tarim block in the India-Asia collision [*Vilotte et al.*, 1984; 1986; *England and Houseman*, 1985] and for the southern termination of the São Francisco craton in the Ribeira belt of southeast Brazil [*Vauchez et al.*, 1994]. Using numerical modeling, these authors conclude that the presence of a stiff block significantly modifies the deformation pattern, leading to strain localization and rotational deformation, even for relatively small viscosity contrasts.

Continental rifting is a process that modifies the thermal profile of the lithosphere over large areas. The final thermal structure is the outcome of two competing processes: an increase in temperatures associated with thinning of the lithospheric mantle and asthenospheric upwelling and an enhanced conductive cooling associated with crustal thinning. For vertically uniform stretching, *England* [1983] has shown that after an initial decrease in the average strength due to lithosphere attenuation, conductive cooling of the lithosphere leads to a rapid increase in lithosphere strength for strain rates $< 10^{-14}s^{-1}$. However, geophysical surveys and petrological studies on rift-related magmatism suggest that in most recent rifts the lithosphere attenuation is larger and affects a wider area than the observed crustal thinning [*Thompson and Gibson*, 1994]. For example, *Davis et al.* [1993] and *Cordell et al.* [1991], on the basis of a tomographic inversion of teleseismic data and gravity surveys in the Rio Grande rift, suggest a total lithospheric thinning ($\beta \sim 2$-4) much larger than the maximum crustal thinning ($\beta < 2$) implied by seismic studies of crustal thickness in this region [*Prodehl and Lipman*, 1989]. Similar results are inferred from gravimetric and seismic surveys in the Baikal rift [e.g., *Zorin et al.*, 1989; *Davis et al.*, 1993], and large-scale multidisciplinary studies in the East African rift [*KRISP Working Group*, 1995, and references therein] suggest the existence of a steep-sided narrow wedge of asthenosphere up to depths of 35-65 km within the rift zone. This enhanced lithospheric attenuation may be explained by additional heat supply at the base of the lithosphere by a hot mantle plume, as has been suggested for the Rio Grande and East African rifts [e.g., *Thompson and Gibson*, 1994; *Achauer et al.*, 1994], or by small-scale convection induced by the large horizontal temperature gradients beneath a passive rift [*Buck*, 1986].

Continental rifts are therefore often characterized by thinner and hotter lithospheres and show reduced strengths. The effect of these weak domains on the mechanical behavior of the continental lithosphere is still poorly understood. Most geological materials, under lithospheric conditions, deform by dislocation creep and show an inverse dependence of strain rates on effective viscosity [e.g., *Chopra and Paterson*, 1981, 1984; *Paterson and Luan*, 1990; *Wilks and Carter*, 1990]. Therefore low-viscosity domains should deform at higher strain rates than the surrounding areas when submitted to similar stresses. This would induce a significant strain localization and development of heterogeneous strain fields in a lithosphere with weak rheological heterogeneities.

The Borborema shear zone system of northeast Brazil (Figure 1) probably results from such a process. It is characterized by a continental-scale array of shear zones developed to accommodate the convergence of the Amazon, São Francisco, and West African cratons. The complex geometry of this intracontinental deformation, in which changes in tectonic pattern are associated with the São Francisco craton and the Orós, Seridó, and Cachoeirinha basins, suggests that intraplate rheological heterogeneities have controlled the mechanical response of the plate to convergence and continental collision.

Based on this natural example, we investigated the perturbation of the first-order kinematic field by intracontinental rheological heterogeneities and, in particular, the effect of these heterogeneities on the development of shear zones through numerical modeling. We have modeled the development of a shear zone associated with a high-viscosity domain (e.g., a craton) in a continental plate subjected to compression, and we have studied how a low-viscosity domain modifies the development of this shear zone. We have also investigated the influence of several parameters, such as the initial viscosity contrast between the weak heterogeneity and surrounding lithosphere, and the location and orientation of the low-viscosity domain on the perturbation of the bulk strain field.

The Borborema Shear Zone System

The shear zone array of the Borborema Province (Figure 1) extends over more than 200,000 km^2. It is formed by NE trending, rectilinear strike-slip shear zones in the western domain and by curvilinear E-W trending transcurrent shear zones terminating in N-S to NE trending metasedimentary belts in the eastern domain [*Vauchez et al.*, 1995]. The complexity of this network raises two problems: Does it form a mechanically coherent system? If so, what processes may lead to such a complex kinematic pattern? Answers to these questions require information on the timing and pressure-temperature (*P-T*) conditions of the deformation within each zone, on the kinematics at the connections between the different high-strain zones (NE and E-W trending shear zones and metasedimentary belts), and on their deformation regimes.

Timing and P-T Conditions of Deformation

Estimates of *P-T* conditions of deformation [*Vauchez et al.*, 1995] suggest that deformation occurred under similar temperature conditions in the entire shear zone array, in which deformation was coeval with partial melting at relatively shallow

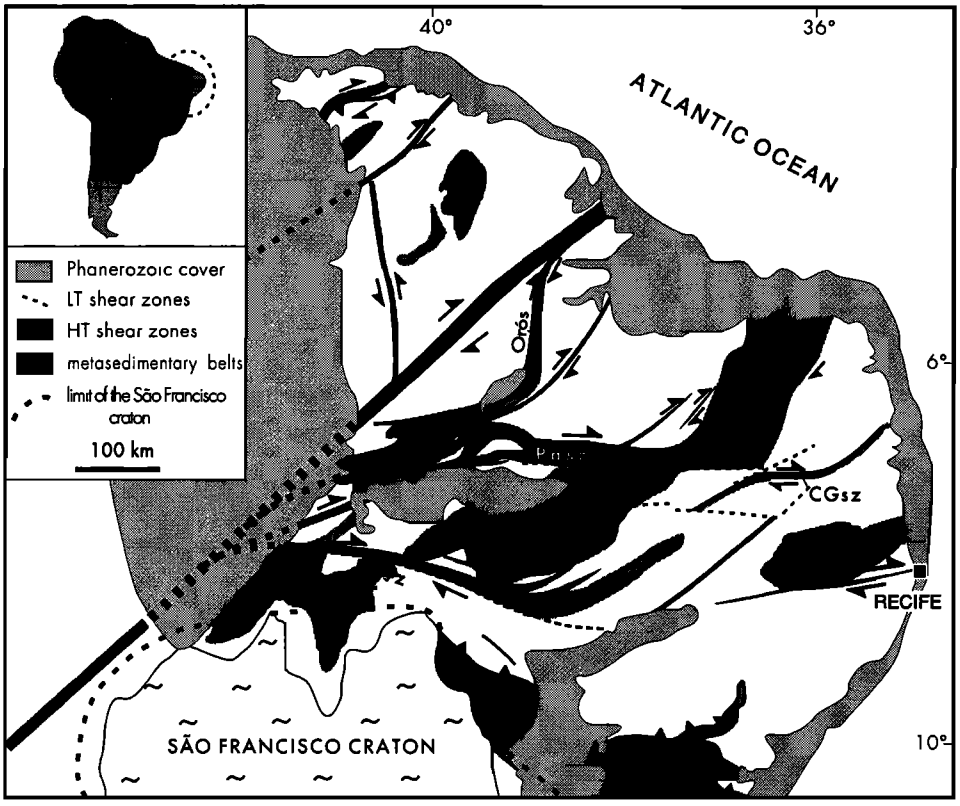

Figure 1. Schematic map of the Borborema shear zone system (location in inset) showing the geometrical distribution of shear zones (black) and metasedimentary belts (dark grey). Abbreviations are Tsz, Tatajuba shear zone; Pesz, West Pernambuco shear zone; Pasz, Patos shear zone; and CGsz, Campina Grande shear zone.

crustal levels (< 20 km depth) and abundant magmatism (partially mantle derived). Higher synkinematic pressure inferred for the western domain points to a greater thickening in this area. Indeed, in the eastern domain, high-temperature, low-pressure conditions prevailed, and $^{40}Ar/^{39}Ar$ analyses indicate a low cooling rate [*Féraud et al.*, 1993].

Available geochronological data [*Sá*, 1991; *Féraud et al.*, 1993; *Leterrier et al.*, 1994] indicate a roughly synchronous deformation over the entire shear zone array. This deformation began at 600-570 Ma and operated intermittently under decreasing temperature conditions until ~ 500 Ma.

Connections Between the Different High-Strain Zones

Continuity between the NE and E-W trending shear zones is observed at the connection of the NE trending Tatajuba with the E-W trending Patos shear zones (Figures 1 and 2). The transition in dominant displacement directions from NE-SW to E-W is accommodated by a 100 km-long arcuate strike-slip duplex structure [*Vauchez et al.*, 1995]. In this area, several lenses of non mylonitized rocks (metasediments, basement gneisses, and igneous bodies) are bounded by kilometer-wide arcuate shear zones. This structure is clearly visible on satellite images (Figure 2), and like horses and duplexes developed in thrust tectonics, it accommodates a change in the main flow direction. *Vauchez et al.* [1995] suggest a similar fault pattern at the western tip of the West Pernambuco shear zone and conclude that the E-W trending shear zones splay off of the NE trending shear zones.

The progressive rotation of structural trend is in agreement with kinematic continuity between the E-W trending shear zones and the deformation within the metasedimentary belts. This is especially well documented in the Patos shear zone-Seridó belt system [*Corsini et al.*, 1991] through satellite images (Figure 2), structural studies, and geophysical data. At the southern tip of the Seridó belt, the lithologic units are progressively bent from NE-SW to E-W, and they enter the Patos shear zone where they are boudinaged. The tectonic fabric progressively rotates from NE-SW to E-W. Structural continuity is also supported by the progressive curvature of the aeromagnetic anomalies [*Moreira et al.*, 1989] that follow the rotation of the tectonic fabric without any discontinuity (Figure 3). Finally, high-temperature mylonites were not observed to the east of the junction between the Patos shear zone and the Seridó belt.

A similar pattern is observed at the connection between the Tatajuba shear zone and the Orós belt (Figures 1 and 2), as well as at the terminations of the Campina Grande and West Pernambuco shear zones. In these zones the high-temperature mylonitic foliation progressively changes orientation over more than 50 km from an E-W to a NE-SW trend and forms a compressional horsetail structure that intimately links the shear zone fabric to the foliation of schists of the Cachoeirinha belt [*Vauchez and Egydio-Silva*, 1992].

Deformation Regimes Within the High-Strain Zones

The simplest mechanical interpretation for an array of contemporaneous shear zones with different orientations is that the array represents a system of conjugate shear zones. However, conspicuous evidence of right-lateral shear in both the NE and E-W trending shear zones precludes this interpretation for the Borborema shear zone system. Moreover, field and microstructural data [*Vauchez et al.*, 1995] indicate that the

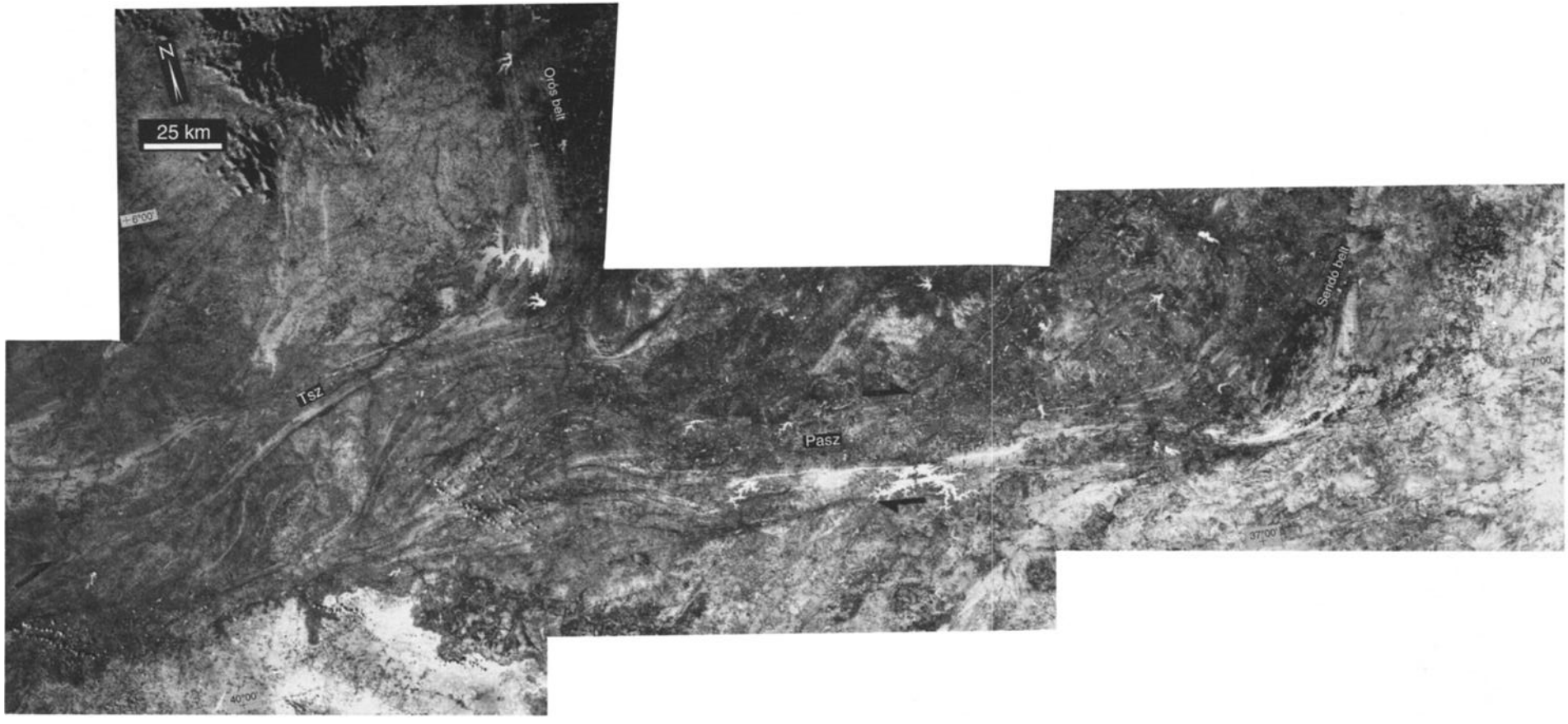

Figure 2. Landsat image of the Patos shear zone (Pasz) showing its connections with the NE trending shear zones and with the Seridó belt. The connection of the Tatajuba shear zone (Tsz) with the Orós belt is also displayed.

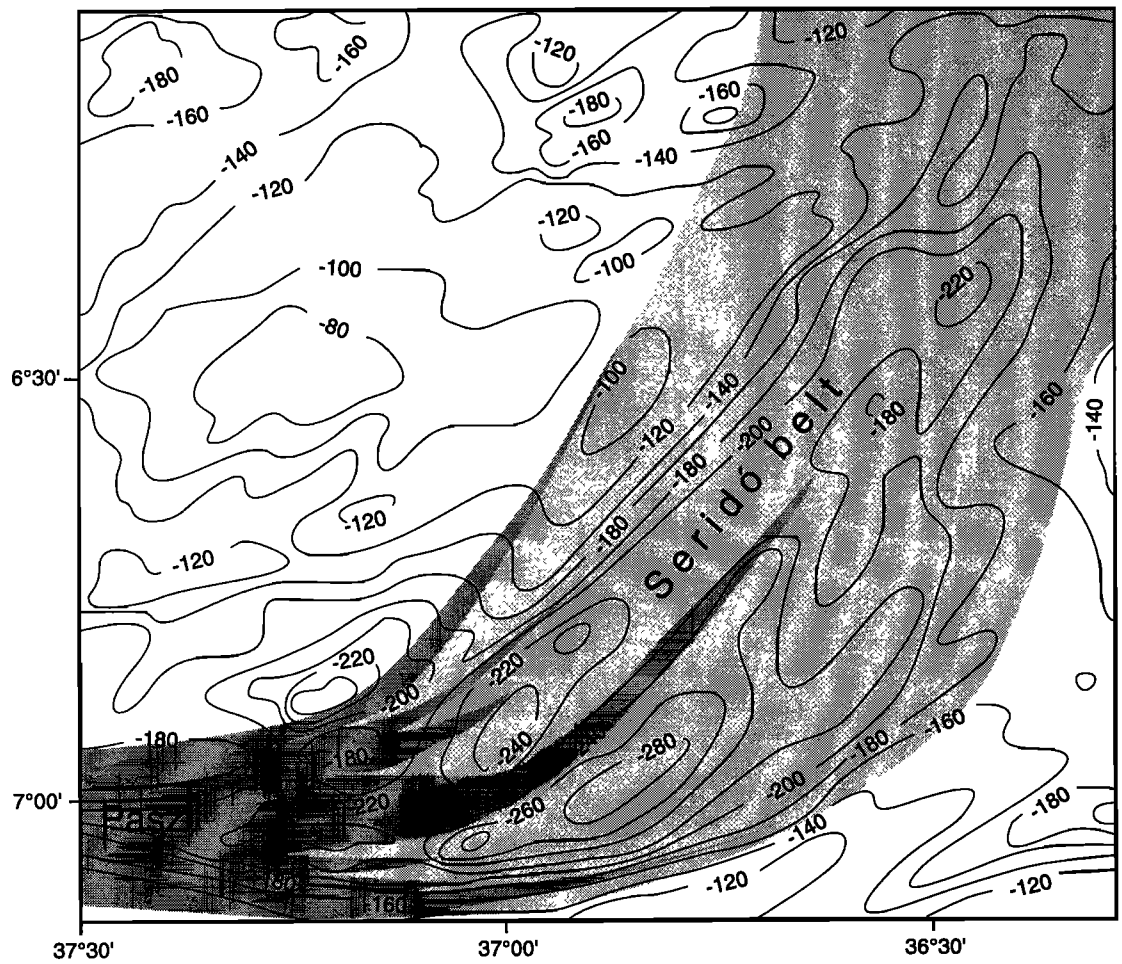

Figure 3. Aeromagnetic map of the connection between the Patos shear zone (Pasz, dark grey) and the Seridó belt (light grey) showing the progressive curvature of the aeromagnetic anomalies that follow the rotation of the tectonic fabric (modified from *Moreira et al.* [1989])

proportion of pure and simple shear within individual shear zones may be related to the shear zone orientation (Figure 4). In the E-W trending shear zones, extensive synkinematic magmatism, in the form of swarms of vertical sills, together with widespread evidence of right-lateral simple shear points to a transtensional deformation. NE trending metasedimentary belts of the eastern domain are characterized by a transpressional deformation, in which strain is partitioned in alternating zones dominated by pure or simple shear. The N-S oriented Orós metasedimentary belt shows predominantly compressive deformation with only subsidiary right-lateral shear zones formed during a late stage of evolution. The observed changes in deformation regime depending on the shear zone orientation are consistent with a single bulk stress field characterized by E-W compression.

What Process Generated Such a Complex Kinematic Pattern?

Considering the continuity between the different high-strain zones (NE and E-W trending shear zones and metasedimentary belts), the similar timing and *P-T* conditions for the deformation in the different branches of the Borborema shear zone system, and the relationship between deformation regimes within individual high strain zones and their spatial orientations, we suggest that this network represents a single, kinematically coherent system formed in response to a homogeneous continental-scale stress field. Heterogeneity of the strain field must therefore have been induced by some intrinsic property of the continental lithosphere.

Recent geochemical data reported by *Brito Neves et al.* [1993] and *Van Schmus et al.* [1993] highlight that the lithosphere of the Borborema Province is heterogeneous. According to these authors, the crust of the central Borborema Province consists of juxtaposed continental domains comprising either an old basement (lower Proterozoic to Archean) or terranes formed around 1.0 Ga during an extensional event which produced large volumes of juvenile crust. Such a "mosaic structure" may account for important horizontal variations of the rheological properties of the lithosphere. It may be expected that the younger terranes, formed during the extensional episode, would display a thinner lithosphere and a higher geothermal gradient, and thus a lower strength, than those sections having an old continental basement. The metasedimentary belts in which the NE trending shear zones terminate are basins formed during this extensional episode; they may therefore have acted as low-strength intraplate heterogeneities during subsequent compressional deformation. This complex rheological structure, with a stiff domain (São Francisco craton) and weak zones (basins), may have led to a heterogeneous mechanical response of the Borborema Province

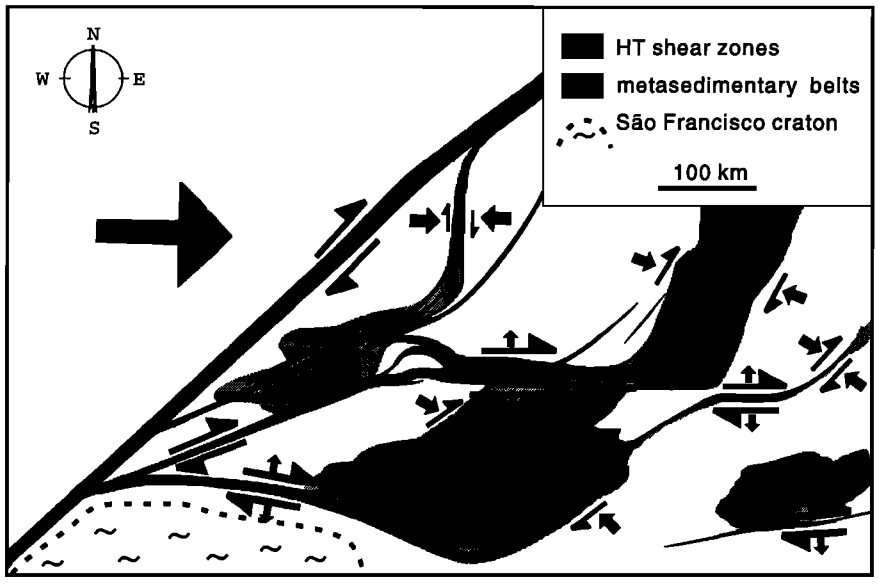

Figure 4. Sketch showing the distribution of deformation regimes in the Borborema shear zone system. The arrows represent the pure and simple shear components of the deformation in the various high-strain zones, and their size indicates the relative magnitude of each component. The large grey arrow indicates the inferred convergence direction.

lithosphere. The basins, in particular, seem to have played an important part in the development of the shear zone system, leading to the initiation and propagation of the E-W trending, sinuous shear zones. These shear zones have subsequently behaved as transfer zones, taking up the deformation between the NE trending shear belt and the basins.

Model

Tectonic studies of the Borborema Province suggest that the kinematic field associated with the shear zone system was controlled largely by the existence of lithospheric-scale rheological heterogeneities. The physical validity of this hypothesis may be investigated by numerical modeling of the mechanical evolution of a rheologically heterogeneous lithosphere subjected to tectonic forces. This approach has already been used to study the effect of a stiff inclusion in convergent environments [*Vilotte et al.*, 1984, 1986; *England and Houseman*, 1985; *Vauchez et al.*, 1994]. However, the influence of low strength domains on the deformation of continental plates has only been studied using vertical plane strain models of extensional environments [e.g., *Dunbar and Sawyer*, 1989; *Chéry et al.*, 1989; *Linch and Morgan*, 1990] and specific compressional environments [*Chéry et al.*, 1991; *Wdowinski and Bock*, 1994], and these studies focused on the effect of heterogeneities on the vertical strain field. We use a two-dimensional mapview model to investigate the influence of a low-strength domain on the finite strain field developed in a continental lithosphere subjected to compression and focus particularly on how this rheological heterogeneity affects the initiation and propagation of shear zones.

The actual Borborema shear zone system is too complex to be modeled directly. We therefore restrict our models to a simplified situation which is similar, though not identical, to the observed tectonic pattern. We investigate the perturbation of a well known reference strain field by the introduction of a single low-viscosity domain (Figure 5). For reference, we used the strain field developed at the termination of a craton subjected to compression, as modeled by *Vauchez et al.* [1994]. This configuration matches the actual geological situation, since the Borborema shear zone system developed at the northern termination of the São Francisco craton (Figure 1). The results of the experiments depend on several parameters, but especially on those related to the configuration of the low strength domain. Thus we investigated the sensitivity of the model to the geometry (the location and orientation of the low-strength zone relative to the converging boundary) and rheology (the viscosity contrast between the low-strength block and the surrounding lithosphere) of the weak domain.

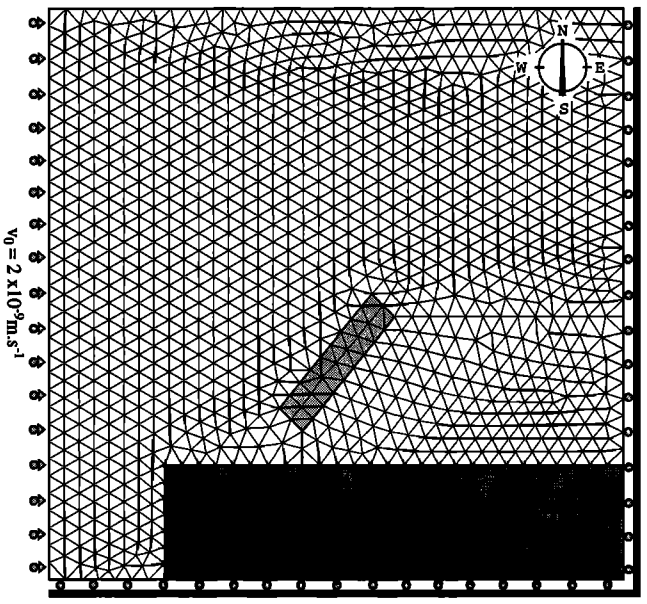

Figure 5. Topology and boundary conditions (represented by engineering symbols) for the models. In the reference model, only the stiff block (dark grey) is added to the "normal lithosphere" (unshaded). In all other models, a low-viscosity block (light grey), representing a basin, is added to the reference configuration.

Geometry and Boundary Conditions

An extreme simplification of the geological situation was used to define the geometry of the numerical model. A quadrilateral plate 2500x2500 km was evaluated on a mesh of 2616 (or 7256, in mesh refinement tests) seven-node isoparametric elements (Figure 5). The rheological heterogeneities were modeled by two quadrilateral blocs: a 500x2000 km stiff block located at the southeastern boundary of the model, representing a craton, and a 500x100 km NE trending, low-viscosity block, corresponding to a basin located in the central domain of the model.

We imposed a constant-velocity eastward displacement on the western boundary of the plate, simulating the convergence of the Amazon with the West African and São Francisco cratons. Since geological constraints on the convergence rate are lacking, in most models the velocity was arbitrarily set to 6 cm y^{-1}; however, tests were also run using lower convergence rates (0.3 and 1 cm y^{-1}). The southern and eastern boundaries were free to glide laterally (reflective conditions), simulating the extension of similar terranes to the south and east of the modeled domain. The northern boundary, for which geological constraints are lacking, was set free to move both parallel and normal to its trace.

Both plane strain and plane stress approximations have been used, but only plane stress results are presented, since this approximation accounts for vertical deformations, especially thickening in the low-strength domains. In these plane stress models, however, vertical deformations are overestimated because gravitational forces are not taken into account in the physical formulation. They correspond to zero Argand number models, as defined by *England and McKenzie* [1982]. Such models may represent an idealized situation in which erosion is extremely effective and counterbalances the excess thickening, hindering the development of significant buoyancy forces. Since plane strain models represent the other limiting case, in which deformation is confined to the horizontal plane, the results of these models are summarized and compared with the results of plane stress models in the discussion.

Physical Formulation

Numerical modeling was performed using a finite-element program developed by *Daudré* [1991] in which a Lagrangian formulation of the equations of continuum mechanics is solved for either plane strain or plane stress approximations. The deformation of the lithosphere is modeled by Stokes flow of a nonlinear, incompressible, viscoplastic material that follows a Norton law and a Von Mises plasticity criterion. Consequently, the constitutive relation is

$$\sigma_{ij} = 2\mu\dot{\varepsilon}_{ij} + \delta_{ij}p \tag{1}$$

where σ_{ij} is the Cauchy stress tensor, $\dot{\varepsilon}_{ij}$ is the strain rate tensor, p is the pressure, and δ_{ij} is the Kronecker delta. The effective viscosity μ for a nonlinear, thermally activated material is defined by:

$$\mu = \left(\sigma_y + \left(\frac{\bar{\dot{\varepsilon}}}{\gamma\sqrt{3}} \right)^{1/n} \right) / \bar{\dot{\varepsilon}}\sqrt{3} \tag{2}$$

where σ_y is the plasticity limit, $\bar{\dot{\varepsilon}}$ is the second invariant of the strain rate tensor, n is the stress exponent, and γ is the fluidity, which depends on the temperature T according to

$$\gamma = \gamma_0 \exp\left(\frac{-Q}{RT} \right) \tag{3}$$

where R is the universal gas constant, γ_0 is a material constant and Q is the activation energy.

Vertically Integrated Rheology

Two-dimensional modeling of large horizontal displacements (strike-slip motions) requires severe simplifications of the rheology of the lithosphere that varies with depth depending on the local geothermal gradient and lithological layering. In mapview models, this vertically heterogeneous rheological behavior must be approached by a single constitutive relation that characterizes a vertically integrated rheology of the lithosphere [e.g., *England*, 1983; *England and Houseman*, 1986, 1989; *Bird*, 1989].

The different domains of the model represent terranes with different continental accretion ages and tectonic histories (i.e., a cratonic domain surrounded by a younger lithosphere in which basins have formed). These domains are characterized by contrasting geothermal gradients and lithospheric thicknesses, and thus display different rheological profiles (Figures 6a, 6b, and 6c). Integration of the deviatoric stress with respect to depth gives the lithospheric strength of each domain, which defines the force per unit length that acts on a vertical lithospheric section to deform the lithosphere at a reference strain rate [*England*, 1983].

Since the lithospheric strength is controlled by the rheology of either the upper mantle, in regions of low to normal geothermal gradients, or the upper crust, in areas of high geothermal gradients (Figure 6), a description of the vertically integrated rheological behavior of the lithosphere that is valid for a large range of geothermal gradients should integrate the contributions of these two layers. This may be approached by a viscoplastic constitutive equation

$$\sigma = \bar{\sigma}_y + \left(\frac{\dot{\varepsilon}}{\bar{\gamma}} \right)^{1/n} \tag{4}$$

where the integrated plasticity limit $\bar{\sigma}_y$ represents the contribution of the upper crust, and the second term corresponds to the contribution of the upper mantle to the lithospheric strength through an integrated fluidity, $\bar{\gamma}$.

Using these vertically integrated rheological parameters, equation (2) becomes

$$\mu = \left(\bar{\sigma}_y + \left(\frac{\bar{\dot{\varepsilon}}}{\bar{\gamma}\sqrt{3}} \right)^{1/n} \right) \bar{\dot{\varepsilon}} / \sqrt{3} \tag{5}$$

The integrated rheological parameters $\bar{\sigma}_y$ and $\bar{\gamma}$ for the different domains of the model (Table 1) were calculated using normalized stresses. These normalized stresses correspond to the depth-averaged stress supported by an homogeneous layer of reference thickness (L = 100 km) that displays a strength equivalent to the calculated lithospheric strength for each domain. The integrated plasticity limit $\bar{\sigma}_y$ corresponds therefore to the normalized stress of the upper crust, and the integrated fluidity $\bar{\gamma}$ is calculated as the fluidity of a homogeneous dunitic layer of thickness L that deforms at a reference strain rate of 10^{-15} s^{-1} when subjected to the normalized stress of the upper mantle.

The calculated strength of the lithosphere and therefore the integrated rheological parameters for the different domains depend on the flow laws used to describe the rheological behavior of the lithosphere with respect to depth, especially those describing the upper mantle rheology. Strength contrasts between the different domains are enhanced for stiff upper mantle

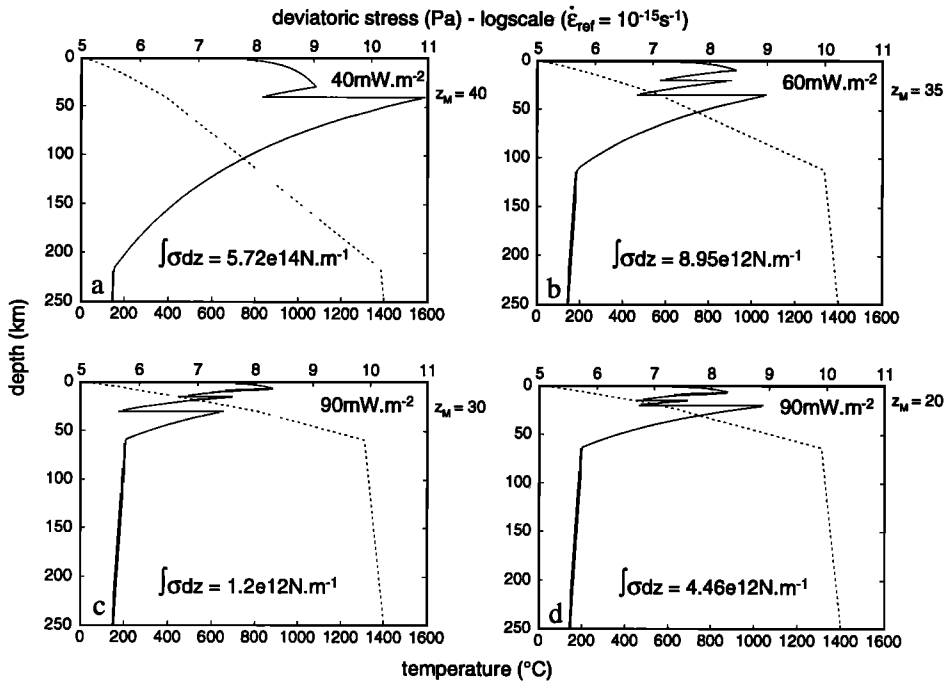

Figure 6. Geothermal gradient (dotted line), one-dimensional strength profile (solid line), and lithospheric strength for different geodynamic settings characterized by typical surface heat flows (top right): (a) a cratonic block, (b) a normal lithosphere, (c and d) a thinned lithosphere. Strength profiles are calculated using *Sibson's* [1974] frictional law for the upper crust, a quartzite flow law [*Paterson and Luan*, 1990] for the quartz-rich upper to middle crust, a felsic granulite flow law [*Wilks and Carter*, 1990] for the lower crust, and the Aheim dunite flow law [*Chopra and Paterson*, 1981] for the upper mantle. For the cratonic block (Figure 6a), the crust is considered as entirely formed by felsic granulite. The Moho depth (in kilometers) is indicated by z_M.

behavior, as obtained using the flow law for dry dunite [*Chopra and Paterson*, 1984]. Thus the integrated rheological parameters for most models were calculated using the wet Aheim dunite flow law [*Chopra and Paterson*, 1981], for which strength contrasts and thus heterogeneities are more subdued.

Results

Reference Model

Compressive deformation of a lithosphere containing a stiff domain (reference model) shows that the presence of a stiff block modifies the otherwise homogeneous deformation field induced by a normal convergence. Strain localization occurs in two domains that are characterized by higher strain rates (Figure 7a): a southwestern domain squeezed between the converging boundary and the stiff block, in which strain is relatively homogeneous, and a wide zone of strain localization initiated at the northwestern corner of the stiff block and extending in a NE direction.

Although the two high-strain domains are continuous, they undergo different deformations. The southwestern domain is subjected to an almost coaxial strain (Figure 7c) characterized by substantial shortening nearly parallel to the convergence direction and by significant vertical displacements related to thickening (Figure 7d). The wide zone that extends from the tip of the stiff domain to the NE displays a large rotational component of strain (Figure 7b), in agreement with right-lateral shear accommodating lateral escape of the material at the free boundary. In the shear zone the principal strain directions are rotated, and the extension axis trends NNE-NE. The vertical finite strain distribution (Figure 7d) shows that significant thickening is restricted to the domain squeezed between the stiff block and the converging boundary and that thickening decreases rapidly away from the stiff block, even though most of the model is subjected to compressive stresses.

Perturbation of the Reference Strain Field by a Less Viscous Heterogeneity

Introduction of a weak heterogeneity induces severe localization of the deformation and significant changes in the geometry and kinematics of the shear zone. The imposed convergence is accommodated, at least partially, by the easier deformation of the less viscous domain. This behavior has a clear influence on the geometrical pattern of the resulting shear zone system. The reference shear zone initiated at the northwestern tip of the stiff block is rotated from its original NE-SW orientation

Table 1. Model parameters

	Definition	Stiff Domain	Main Lithosphere	Weak Domain
σ_y, Pa	plasticity limit	1.62×10^{8}	1.35×10^{7}	5.97×10^{6}
γ, Pa^{-n} s^{-1}	fluidity	1.46×10^{-59}	1.02×10^{-50}	1.24×10^{-49}
n	stress exponent	4.5	4.5	4.5

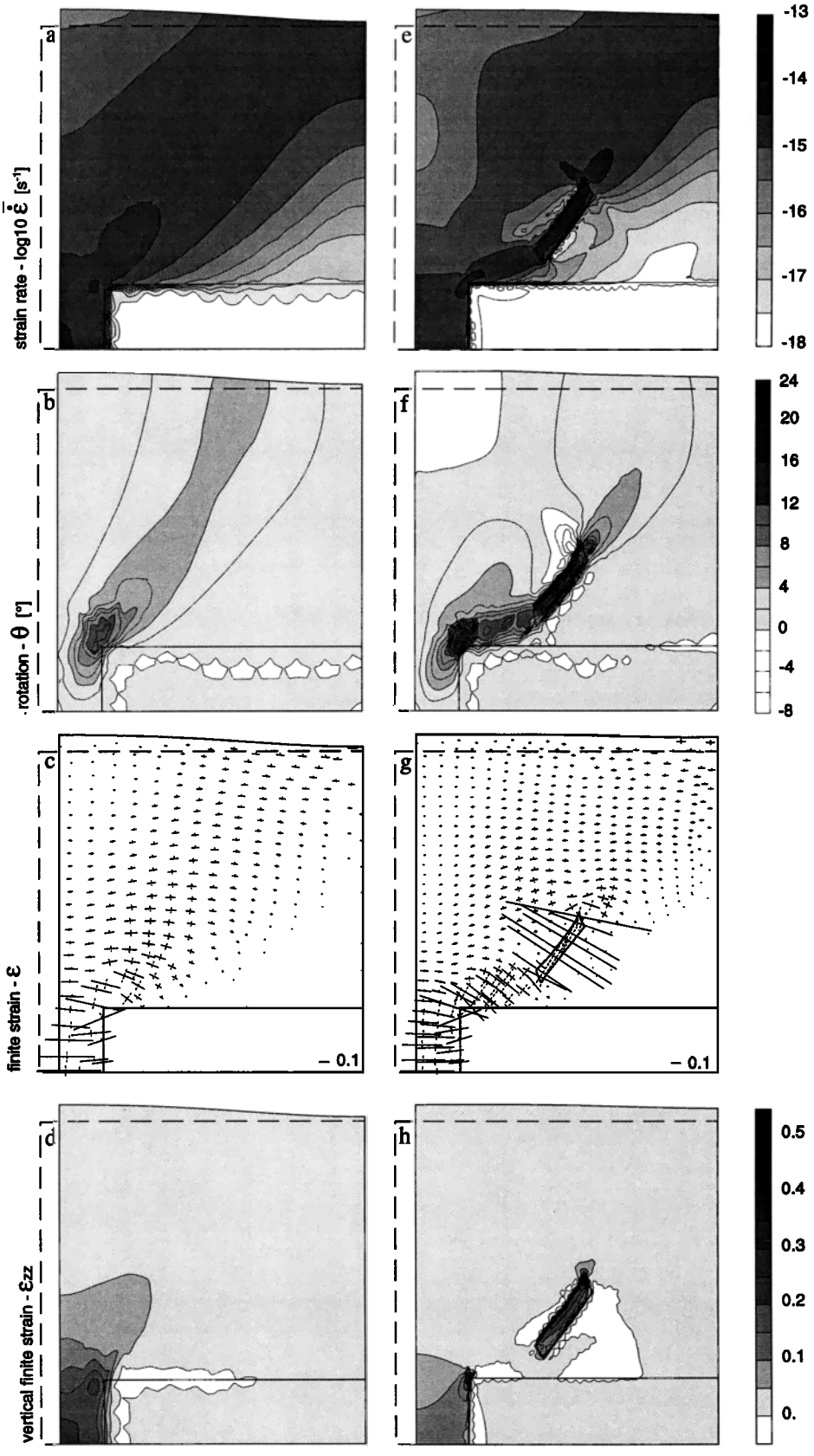

Figure 7. Results after 150 km of convergence: (a-d) for the reference model and (e-h) for a model with a weak domain. Figures 7a and 7e show the second invariant of strain rate tensor. Figures 7b and 7f show finite rotation contours; counterclockwise rotations are displayed in white. Figures 7c and 7g show principal finite strains (Almansi-Euler tensor), solid lines mark shortening directions, and dashed lines indicate stretching directions. Figures 7d and 7h show contours of vertical finite strain; thinned regions are displayed in white.

and extends toward the southern tip of the weak domain (Figure 7e); it becomes a zone of strain transfer linking the northwestern tip of the stiff block with the weak domain.

The rotational deformation is enhanced when a weak block is present (Figure 7f). A right-lateral shear component is clearly related to the high strain rate zones, with maximum shearing related to inflections in the trend of the shear zone at the tip of the stiff block and at the northern termination of the weak domain. Locally, subsidiary left-lateral rotations are induced by kinematic continuity constraints associated with the greater deformation of the less viscous domain relative to its surroundings.

The simple vertical deformation exhibited by the reference model is significantly modified. Vertical finite strain contours (Figure 7h) indicate large thickening within the weak domain that was accompanied by limited thinning to the east and west of this domain, which is possibly related to the imposed kinematic continuity constraints.

A plot of the principal directions of the Almansi-Euler finite strain tensor (Figure 7g) shows that although the pure shear domain remains almost unchanged, elsewhere the finite horizontal strain field is strongly modified by the presence of a weak domain. The high strain values in the low-viscosity domain support that it accommodates a large part of the convergence. The continuity of deformation between the transfer zone and the weak domain is characterized by a continuous change in orientation of the stretching direction from NE in the transfer zone to NNE in the weak domain.

An analysis of the three-dimensional finite strain field shows that whereas the transfer zone deforms by right-lateral simple shear, deformation in the weak domain is transpressive. It is characterized by significant normal shortening and thickening accompanied by limited right-lateral shearing, as is evident from the misorientations of the horizontal stretching direction and the elongation of the basin in Figure 7g. Although the largest stretching (X axis of the finite strain ellipsoid) within the low strength domain is vertical, the magnitude of horizontal stretching is significant. If gravity forces were taken into account, the principal stretching direction would probably be almost basin-parallel.

Sensitivity Studies

We explored the influence of several parameters on the observed perturbation of the reference displacement field. Two types of parameters were studied: the geometrical characteristics of the less viscous domain (involving both orientation and location), and the viscosity contrast between the weak heterogeneity and surrounding lithosphere.

Orientation of the Low -Viscosity Domain

The low-viscosity domain was set with its long edge parallel (E-W), normal (N-S), or at 45° (NE-SW) to the imposed convergence (Figure 8). The initial viscosity contrasts between the different domains were kept constant throughout this series of experiments.

The orientation of the weak domain relative to the bulk convergence direction controls the stress and strain fields within this domain. Convergence-normal basins are subjected to a compressive stress field that induces a dominant pure shear regime characterized by shortening normal to the basin (Figure 9), accommodated mostly by thickening (Figure 10) and subsidiary right-lateral shearing (Figure 11). Along a traverse from the transfer zone to the basin, the stretching direction

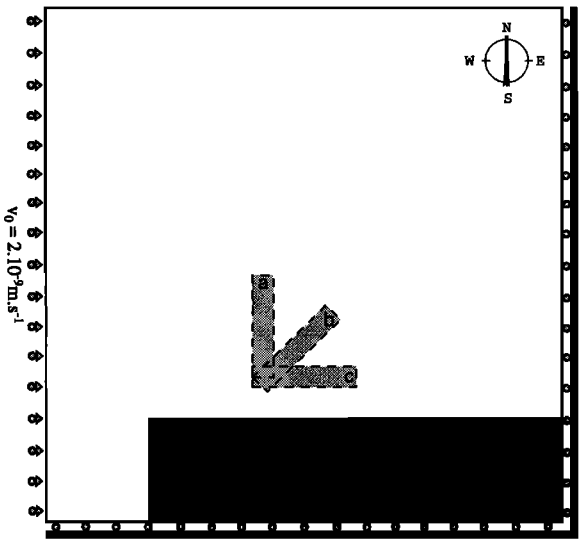

Figure 8. Topology and boundary conditions for models investigating the effect of the orientation of the low-viscosity domain. Boundary conditions and location of the stiff block (dark grey) are the same as in preceding models. The low viscosity domain (light grey) is set in the various experiments either normal (domain a), oblique (domain b), or parallel (domain c) to the imposed convergence direction.

(Figure 9) is progressively rotated toward a N-S direction, suggesting a decrease in right-lateral shearing relative to shortening within the basin away from the transfer zone. Convergence-oblique basins are characterized by a transpressive deformation in which significant right-lateral shearing (Figure 11) is associated with thickening (Figure 10), whereas convergence-parallel basins are subjected to a transtensional deformation that induces right-lateral shearing (Figure 11) and moderate thinning (Figure 10) within the basin.

Convergence-parallel basins seem less efficient in the accommodation of deformation than basins with other orientations, as the original shear zone is only partially deflected into the weak domain, whereas in convergence-oblique and -normal basins the deformation is completely transferred to the basin by an E-W oriented shear zone (Figure 11). Strain propagation seems inefficient within convergence-parallel basins. This may account for the heterogeneous deformation of the basin, which displays a greater right-lateral shearing within its western domain.

Location of the Low-Viscosity Domain

The effect of the location of the low-viscosity domain on the system behavior was studied by placing the western tip of the weak zone at 250, 500, 750, and 1000 km from the western termination of the stiff block (Figure 12). The initial viscosity contrasts between the different domains were kept constant throughout this series of experiments.

The location of the low-strength domain relative to the shear zone initiated at the tip of the stiff block affects the strain rate and finite strain fields (Figure 13), since the amount of deformation accommodated by the weak domain is inversely proportional to its distance from the shear zone. In models for which the weak heterogeneity is located within 500 km of the NW corner of the stiff block ("near" basin models), the NE trending shear zone originating at the corner of the stiff domain is completely reoriented toward the weak block. As this shear zone extends out

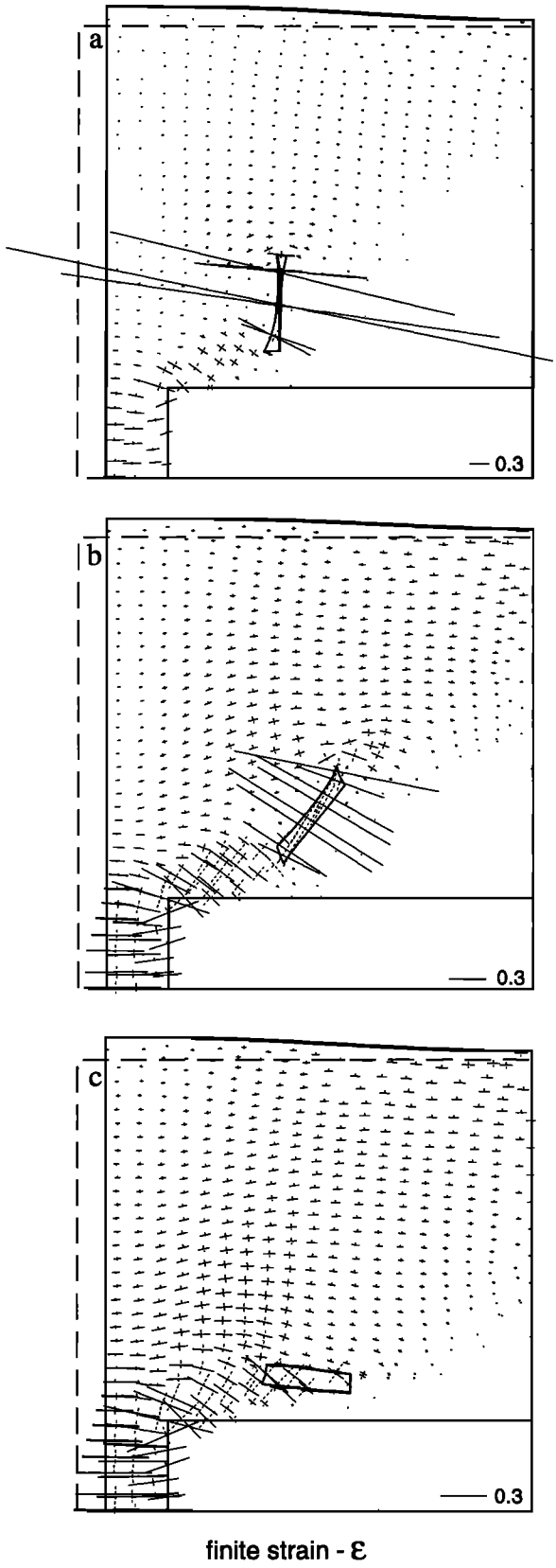

Figure 9. Effect of the orientation of the low-viscosity domain on the finite strain; principal finite strains (Almansi-Euler tensor) after 150 km of convergence for models with (a) a convergence-normal basin, (b) a convergence-oblique basin, and (c) a convergence-parallel basin. Solid lines mark shortening directions, and dashed lines indicate stretching directions.

of the weak domain, it tends to recover its original NE orientation. However, in models for which the weak domains are located farther than 500 km from the NW corner of the stiff domain ("far" basin models), the NE trending shear zone initiating at the tip of the stiff block is not completely deflected. It splits into two branches: one follows its original NE-SW trend, while the other displays a sharp bend toward the southern tip of the weak domain and defines a zone of strain transfer connecting the northwestern corner of the stiff block to the weak domain. For distances approaching 1000 km, strain seems to be equally distributed between both branches.

Finite rotation contours (Figure 14) also allow the evaluation of the relationship between the position of the weak zone and its ability to accommodate the deformation. In near basin models, all rotational deformation generated at the tip of the stiff block is directed to the weak domain, whereas in far basin models, only part of the rotational deformation is transferred to the weak domain. Moreover, the amount of subsidiary counterclockwise rotation decreases with increasing distances.

Initial Viscosity Contrast

The effect of the initial viscosity contrast between the low-viscosity domain and the surrounding terranes was examined for a NE oriented low-viscosity domain located 500 km away from the northwestern tip of the stiff block. The integrated rheological parameters $\bar{\sigma}_y$ and $\bar{\gamma}$ for the weak domain were successively calculated for different geothermal gradients and lithospheric thicknesses, characterized by surface heat flows of 70, 75, 80, and, 90 mW m^{-2} (Figure 15). For the other domains, the rheological parameters were kept constant and were calculated using surface heat flows of 40 mW m^{-2} for the stiff block and 60 mW m^{-2} for the main domain (Table 1). These thermal gradients imply varying viscosity contrasts between the weak domain and its surroundings ; for a constant strain rate of 10^{-15} s^{-1}, the ratios of viscosity of the surroundings relative to the weak domain take on values of ~ 1.5, 3, 5, and 9, respectively.

The viscosity contrast between the different domains has a marked influence on the response of the system to convergence (Figure 16) because it controls the relative ability of the domains to localize the deformation. Models with low initial viscosity contrasts display a branched shear zone system similar to the one observed in the far basin models. As the initial viscosity contrast is increased, an increasing amount of the deformation is concentrated in the weak domain; the NE oriented branch of the shear zone tends to be annihilated. Higher viscosity contrasts also increase strain transfer along the weak block, leading to the initiation of a new NE trending right-lateral shear zone at its northeastern tip.

The rotational deformation is intensified in models with higher viscosity contrasts (Figure 17). Rotational deformation is progressively localized within narrower zones. As strain within the low-viscosity domain increases in models with high initial viscosity contrasts, strain compatibility constraints induce stronger subsidiary left-lateral rotations in these models. Vertical strains, especially thickening in the weak domain, are also intensified in models with high viscosity contrasts.

Discussion

Regardless of its geometrical characteristics, a low-viscosity heterogeneity induces a significant perturbation of the finite strain field. Accommodation of convergence by the less viscous domain enhances strain localization and induces significant

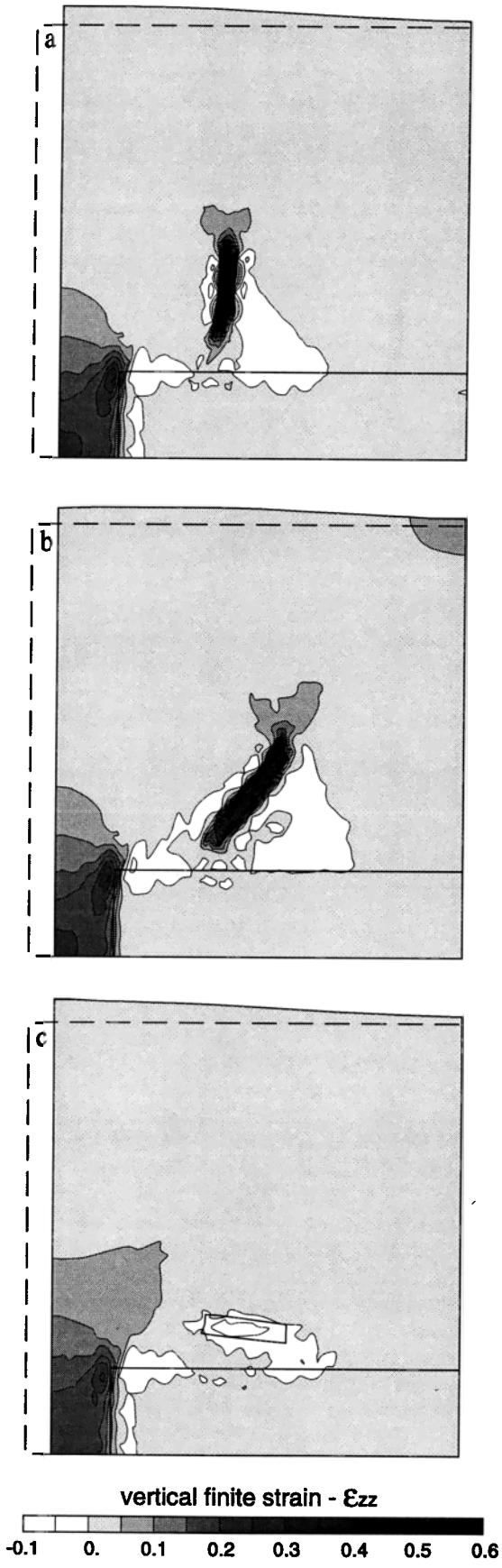

Figure 10. Effect of the orientation of the low-viscosity domain on the vertical finite strain after 150 km of convergence for models with (a) a convergence-normal basin, (b) a convergence-oblique basin, and (c) a convergence-parallel basin. Thinned regions are displayed in white.

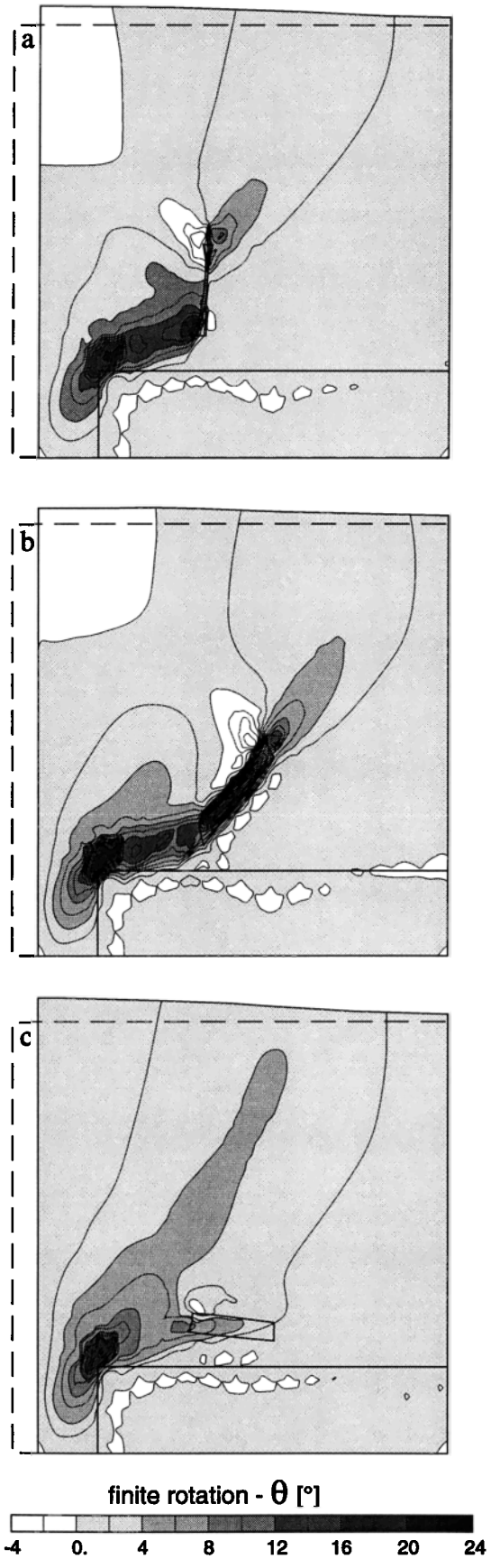

Figure 11. Effect of the orientation of the lo v-viscosity domain on the rotational deformation after 150 km of convergence for models with (a) a convergence-transverse basin, (b) a convergence-oblique basin, and (c) a convergence-parallel basin. Regions showing counterclockwise rotations are displayed in white.

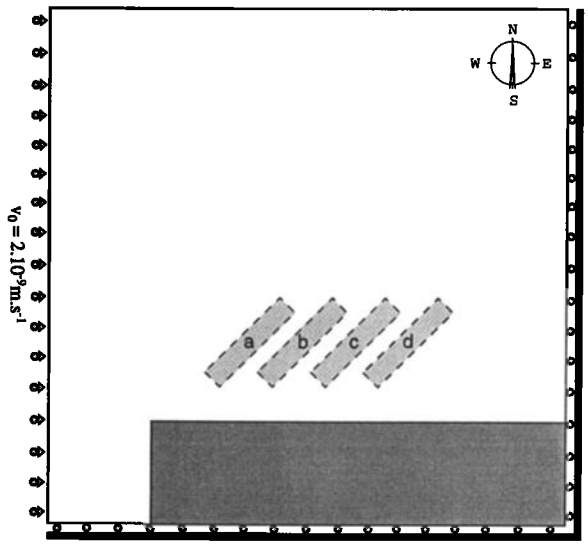

changes in the shear zone pattern. Most geological materials under lithospheric conditions deform by dislocation creep and display a nonlinear behavior characterized by shear thinning, i.e., an inverse dependence of the effective viscosity on the strain rate. Strain localization in the low-viscosity domain induces a further reduction in viscosity within this domain, increasing the viscosity contrast. This behavior has a strong effect on the location and orientation of the high-strain zones and may lead to finite strain fields displaying complex geometrical patterns. The shear zone initiated at the northwestern corner of the stiff block is either

Figure 12. Topology and boundary conditions for the models investigating the effect of the location of the low viscosity domain. Boundary conditions and location of the stiff block (dark grey) are the same as in preceding models. The low viscosity domain (light grey) is set in the various experiments at 250 km (domain a), 500 km (domain b), 750 km (domain c), and 1000 km (domain d) from the western termination of the stiff block.

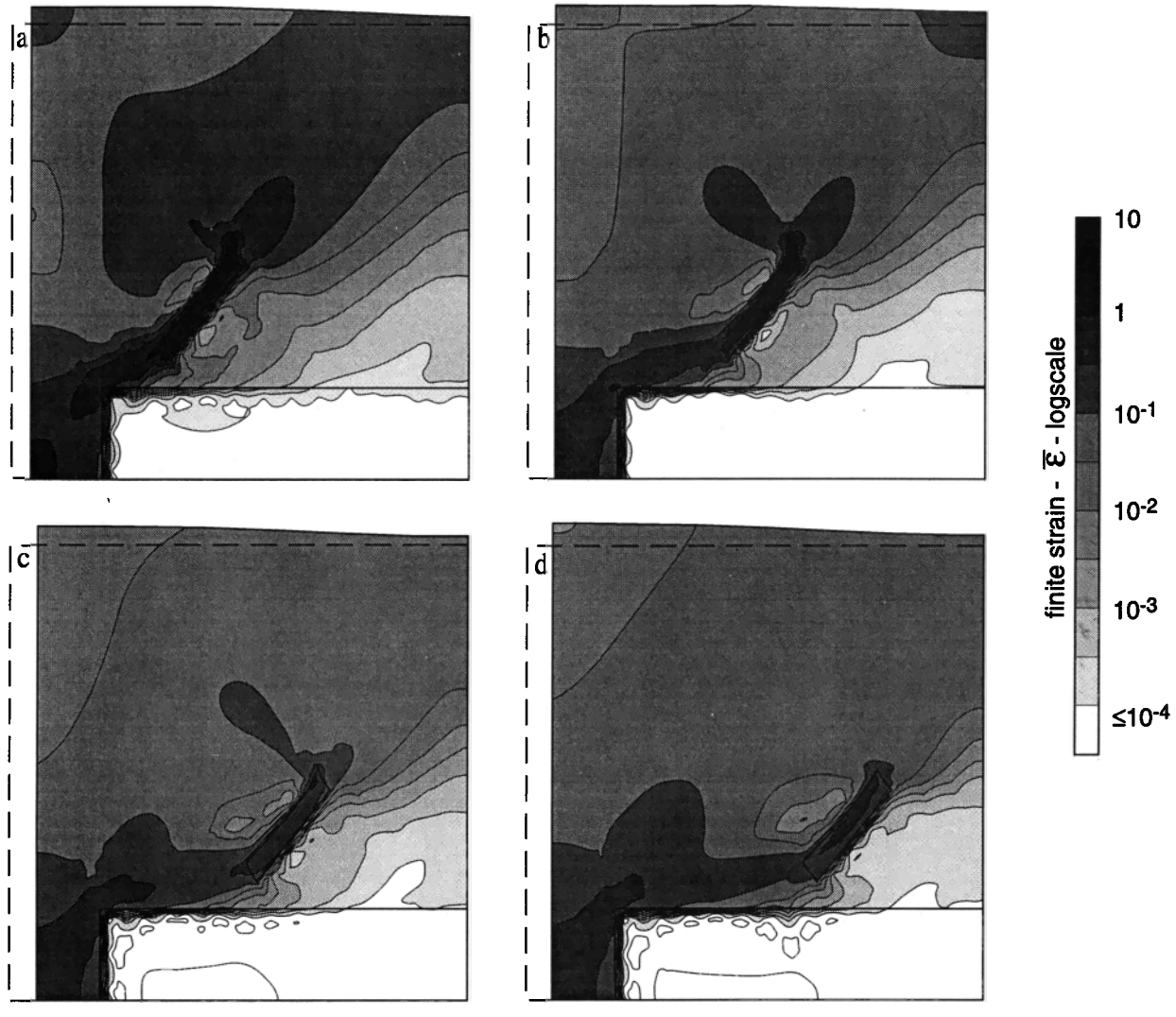

Figure 13. Effect of the location of the low-viscosity domain on strain localization: contours of the second invariant of the Almansi-Euler finite strain tensor (logarithmic scale) after significant convergence (150 km for all examples except Figure 13a) for models with a basin located at (a) 250 km, (b) 500 km, (c) 750 km, and (d) 1000 km of the termination of the stiff block. Results for Figure 13a are displayed for 120 km of convergence because of mesh problems at larger amounts of convergence.

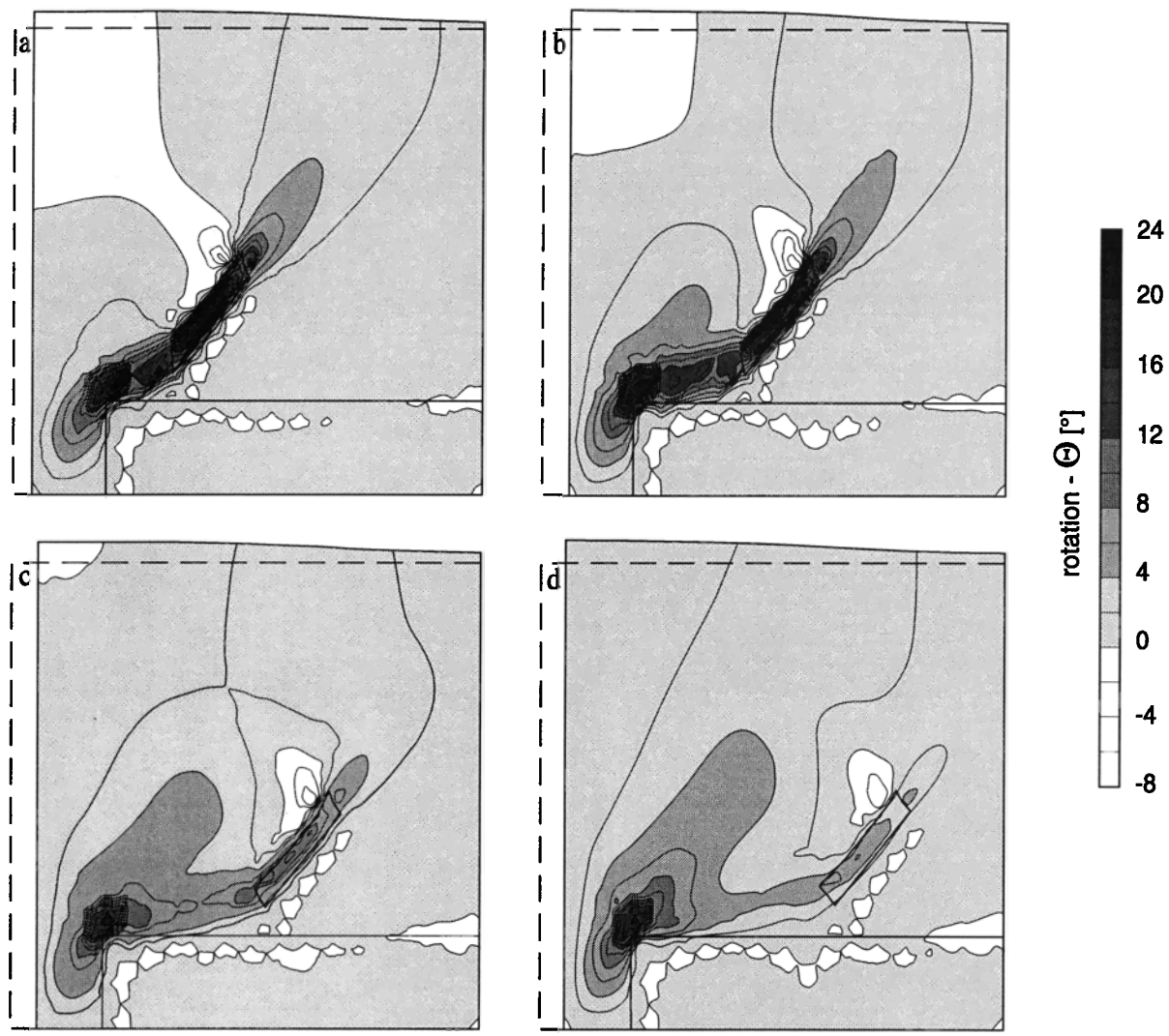

Figure 14. Effect of the location of the low viscosity domain on rotational deformation; finite rotation contours after significant convergence (150 km for all examples except Figure 14a) for models with a basin located at (a) 250 km, (b) 500 km, (c) 750 km, and (d) 1000 km of the termination of the stiff block. Regions showing counterclockwise rotations are displayed in white. Results for Figure 14a are displayed for 120 km of convergence because of mesh problems at larger amounts of convergence.

split, forming a branched shear zone system, or completely rotated from its original NE-SW orientation toward the southern tip of the weak domain. The E-W trending branch acts as a strain transfer zone that links the northwestern tip of the stiff block to the southwestern corner of the weak domain.

The magnitude of the perturbation of the strain field depends on the ability of the weak domain to localize the deformation. The initial viscosity contrast and the distance between the weak domain and the termination of the stiff block have clear quantitative effects, since they affect the amount of deformation accommodated by the low-viscosity domain. The orientation of the weak domain relative to the bulk convergence direction has a qualitative effect; in particular, it controls the deformation regime within the low-viscosity domain. The kinematic field is also affected by the initial viscosity contrasts between the weak domain and the surrounding terranes; in models with low viscosity contrasts, the shear zone formed at the tip of the stiff domain is split, while in models with large viscosity contrasts, the shear zone is completely rotated toward the weak domain.

To check the stability of the numerical solutions, we tested the effect of the imposed boundary conditions. A few experiments have been performed using a plane strain approximation. In this case the ability of the low-strength domain to accommodate the deformation efficiently is minimized. Notwithstanding this result, the finite strain field in the plane strain experiments is significantly perturbed by the presence of a weak domain oriented favorably for shearing (i.e., convergence-oblique basins). The shear zone originating at the termination of the stiff block branches into two well-developed independent shear zones; one follows the original NE trend, and the other extends toward the weak domain.

The effect of the free boundary was investigated by restraining displacements normal to its trace; this condition precludes the northward escape observed in preceding models. Although the northeastward propagation of the shear zone initiated at the tip of the stiff block is hindered, the effect of a low-strength domain on the mechanical response of the lithosphere does not depend on the presence of a free boundary. As in the preceding models, the

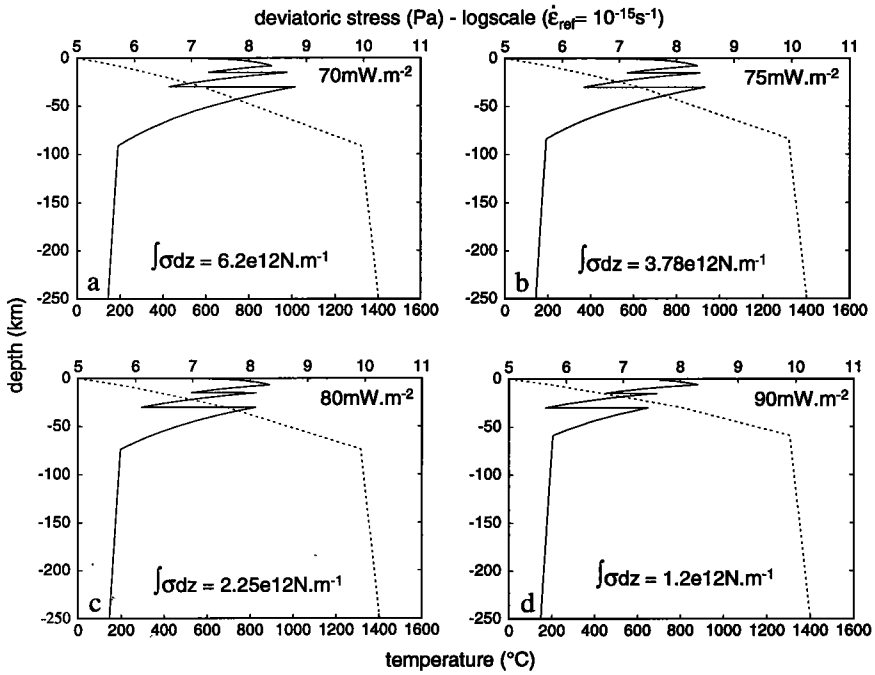

Figure 15. Lithospheric strength of the weak domain calculated for various geothermal gradients (corresponding surface heat flows at upper right). Strength profiles are calculated using the same flow laws as in Figure 6.

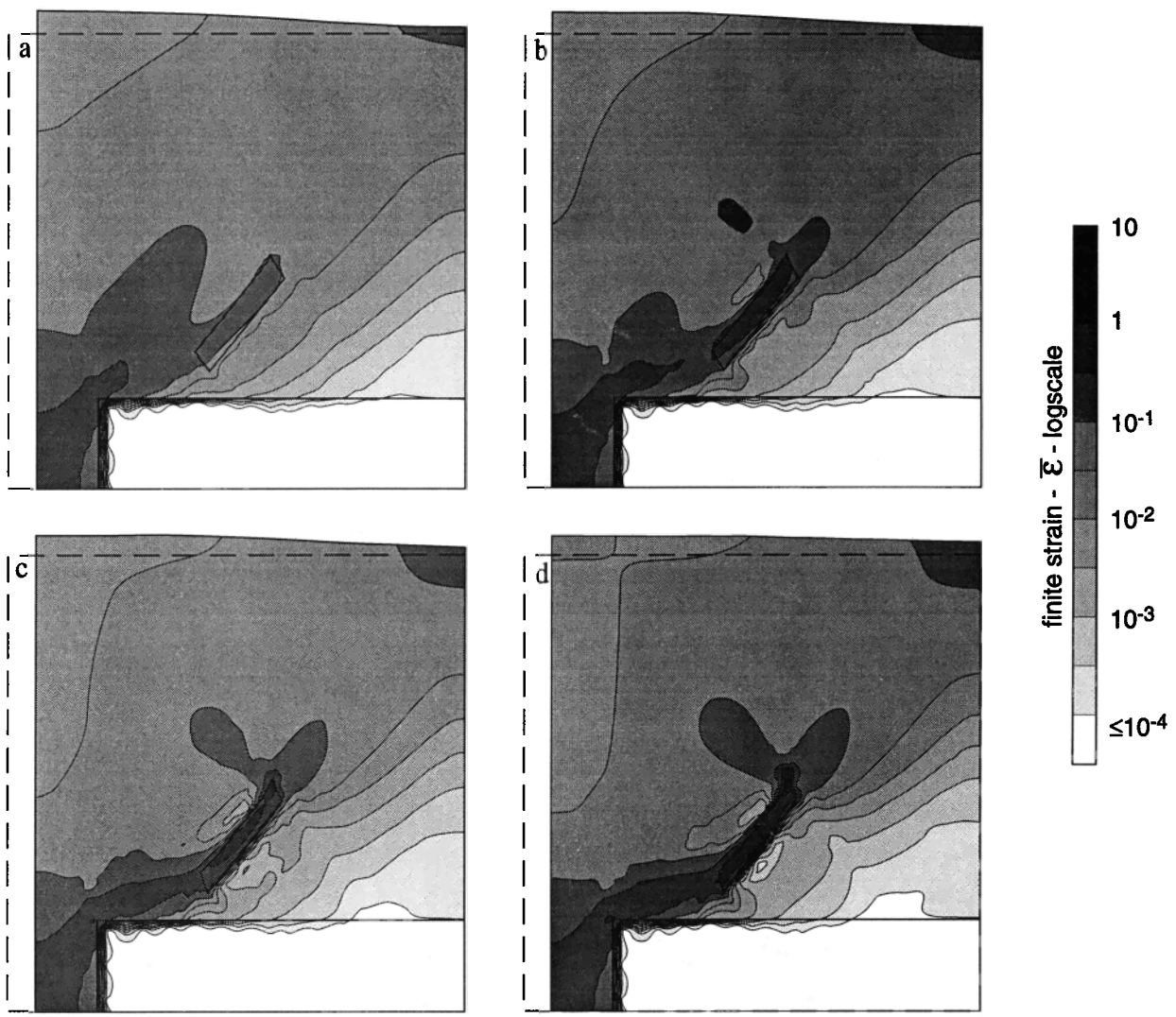

Figure 16. Effect of the initial viscosity contrast between the weak domain and the surrounding lithosphere on strain localization: contours of the second invariant of the Almansi-Euler finite strain tensor (logarithmic scale) after 150 km of convergence. Integrated rheological parameters for the weak domain are calculated using the strength profiles of Figure 15a, Figure 15b, Figure 15c, and Figure 15d, respectively. The rheological parameters for the other domains are kept constant.

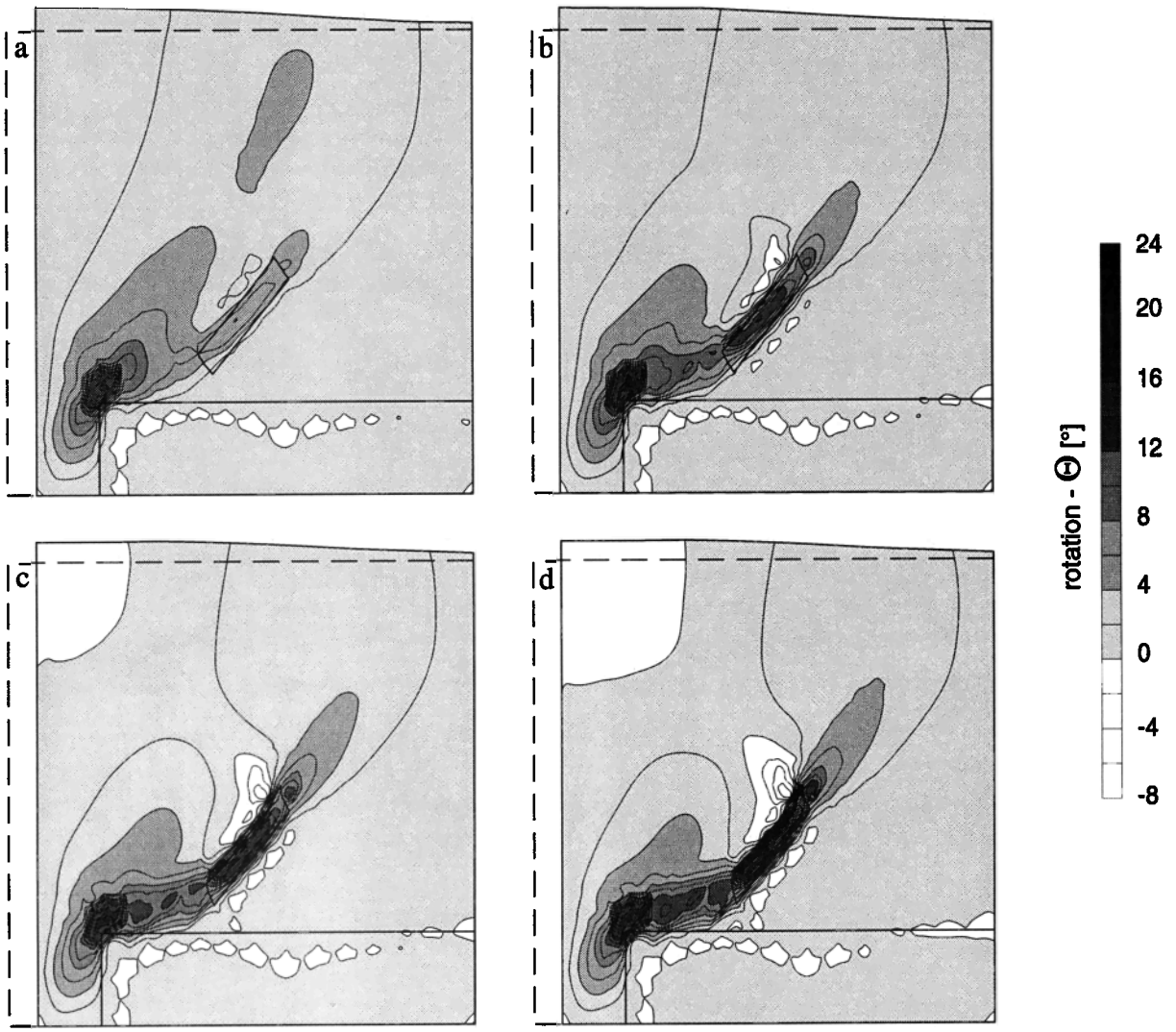

Figure 17. Effect of the initial viscosity contrast between the low-viscosity domain and surrounding areas on rotational deformation: finite rotation contours after 150 km of convergence. Regions showing counterclockwise rotations are displayed in white. Integrated rheological parameters for the weak domain are calculated using the strength profiles of Figure 15a, Figure 15b, Figure 15c, and Figure 15d, respectively. The rheological parameters for the other domains are kept constant.

right-lateral shear zone is rotated toward the weak domain and serves as a strain transfer zone. Vertical strains, especially within the low-strength domain, are clearly increased.

We also tested the effect of the imposed convergence velocity by varying this velocity from 6 cm y^{-1} to 1 or 0.3 cm y^{-1}. Although the strain rate and vorticity fields display a dependence on the convergence velocity (models with higher convergence velocities display higher strain rates and vorticities), for a fixed amount of convergence (i.e., for similar displacements at the model eastern boundary), the finite strain and rotation fields are not affected by variations of the imposed convergence velocity. Finally, the stability of the numerical solution was tested by mesh refinement, using a model with 7256 elements, with consistent results.

The numerical modeling presented here does not address the tectonic evolution of a specific area but rather evaluates specific physical processes that may be invoked to explain observed natural deformations. Nevertheless, a discussion of the modeling results with reference to the Borborema shear zone system may give insights on whether these physical processes may represent active geodynamical processes.

The western domain of the Borborema shear zone system is characterized by large-scale NE oriented, right-lateral shear zones forming a major transcurrent deformation zone. This zone fits well the NE trending, right-lateral shear zone initiated at the northwestern tip of the stiff block in the models. The Borborema shear zone system is also characterized by sinuous E-W oriented right-lateral shear zones that splay off from the NE trending shear belt and terminate in N-S to NE trending metasedimentary belts; this curvilinear geometry is marked by a progressive rotation of foliations and stretching lineations. In the models the shear zone initiated at the northwestern tip of the stiff block tends to be partially or completely rotated from its original NE-SW orientation toward the southern tip of the weak domain and serves as a zone of strain transfer linking the northwestern tip of the stiff block and the weak domain. A progressive rotation of the principal directions of finite strain from the strain transfer zone to the weak domain is also observed in the models.

The deformation in the Borborema shear zone system is characterized by (1) a right-lateral transtension in the E-W oriented shear zones, (2) a right-lateral transpression in NE oriented metasedimentary belts (e.g., Seridó belt), and (3) a dominant belt-normal shortening regime in the N-S oriented basin (Orós belt). The strain regimes within the metasedimentary belts are well represented in the models; the low-viscosity domains experience thickening and right-lateral shearing in proportion to their obliquity to the convergence direction, as is observed in the metasedimentary belts. However, the strain transfer zones of the models deform by simple shear and do not display the associated extensional deformation observed within the E-W trending shear zones of the Borborema Province. This incongruity could result either from the slight obliquity of the transfer zones in the models to the convergence direction or from a weaker rheological behavior of the E-W trending shear zones than that modeled, since low-viscosity domains oriented parallel to the convergence display a transtensional deformation.

The similarity of natural and modeled deformation fields supports the hypothesis that the Borborema shear zone system may have developed by deformation of an heterogeneous continental lithosphere. The NE-trending shear belt of the western domain may have been promoted by the interaction of the convergence process with the lithospheric-scale heterogeneity represented by the termination of the São Francisco craton, which is much older than the surrounding Borborema Province, and represents a thicker, cooler, and thus stiffer lithosphere [e.g., *James et al.*, 1995; *Vitorello et al.*, 1980]. The sinuous geometry of the eastern Borborema shear zone system may have been induced by weak preorogenic basins. Deformation of these domains may have triggered the formation of E-W shear zones connecting the NE trending shear belt originated at the termination of the craton and the basins. Thus perturbation of the mechanical behavior of the continental lithosphere by intraplate rheological heterogeneities not only is physically possible but may also represent an active geodynamic process responsible for development of complex natural deformation patterns.

An essential parameter that needs further investigation is the period of time that rheological heterogeneities characterized by high geothermal gradients can be maintained. Once rifting ceases, the thermal anomaly associated with a basin decays as heat is dissipated by conduction, both vertically to the surface and laterally to the colder surrounding terranes. Therefore significant perturbations of the strain field by the existence of a thermal anomaly associated with a basin seems possible only during a limited time span following the period of extension. This time span depends on the initial thermal anomaly, on the volume of juvenile crust created, on the amount of lithosphere affected by extension, and on the synrifting and postrifting subsidence and sedimentation history. Numerical models of the thermal evolution of continental lithosphere affected by tectonic events [*Sahagian and Holland,* 1994] indicate that a thin lithosphere tends to display a more rapid thermal evolution than does a thick lithosphere but that the thermal evolution slows with progressive thickening of the lithosphere. Moreover, subsidence and sedimentation tend to thicken the crust within basins. Our models show that for low geothermal gradient variations ($\Delta q_s \sim 10$ mW m^{-2}), and small contrasts in crustal thickness between the low-viscosity domain and surrounding lithosphere, the finite strain field is still affected, although moderately, by the weak domain. Thus significant strength contrasts may persist for large time spans (≥ 100 m.y.).

Finally, a question that may arise concerns the application of model results obtained using a constitutive relation based largely on the upper mantle rheological behavior to the whole lithosphere. The similarity between the deformation observed in the middle to lower crust of the Borborema Province with the finite strain fields of the models suggests that the uppermost mantle and lower crust may have deformed coherently in response to plate convergence. This would indicate small strength variations between the two layers, in agreement with a mafic to ultramafic composition of the lower crust as suggested by eclogites described in a few areas [*Beurlen et al.*, 1992]. Moreover, both the upper mantle and lower crust were probably partially molten during deformation, as inferred from *P-T* studies on synkinematic minerals [*Vauchez and Egydio-Silva*, 1992] and from the emplacement of mantle- and crust-derived synkinematic magmas [*Neves and Vauchez,* 1995]. However, the kinematic pattern modeled may not extend far down into the mantle. The asymptotic behavior of the effective viscosity with increasing temperatures implies a reduction of the viscosity contrast at high temperatures. This suggests that the perturbation induced by preexisting basins may be negligible in the deeper levels of the lithosphere, where the effect of a cratonic block with its deep and cold root may still be important. A possible consequence could be a variation in kinematic pattern with depth, with lower layers of the lithosphere showing a more homogeneous NE trending flow.

Conclusion

Continental plates are rheologically heterogeneous media because they grow through the amalgamation of domains with different continental accretion ages and tectonic histories. Numerical modeling shows that the presence of low-viscosity heterogeneities as well as of stiff heterogeneities produces significant perturbations of the finite strain field. Accommodation of the convergence by deformation of the less viscous domain induces pronounced strain localization and large modifications of the geometry of the high-strain zones. As viscosity of nonlinear materials is highly dependent on strain rate, strain localization in the weak domain triggers further increases in viscosity contrasts and thus enhances the initial heterogeneity. The perturbation of the strain field depends on the ability of the weak domain to accommodate the deformation. The initial viscosity contrast, the orientation of the weak domain relative to the bulk convergence, and its distance from the shear zone initiated at the termination of the stiff block represent important parameters that govern the response of the model.

The mechanical response of continental plates to plate tectonic processes should therefore result from an interplay between the boundary conditions imposed by plate motions and the effects of heterogeneities within the continental lithosphere. The resulting finite strain field integrates this interaction, and complex kinematic patterns may develop. A heterogeneous continental plate subjected to a normal convergence may therefore display a highly heterogeneous strain field, as is exhibited by the Borborema shear zone system, in which intraplate heterogeneities induce the development of branched or sinuous shear zones. Significant lateral variations in strain intensity, deformation regimes, and vertical strains may also occur and give rise to contrasting metamorphic and uplift histories.

Acknowledgments. We thank Jean Chéry for numerous discussions and suggestions, and Raymond Russo, Gregory Houseman, and Andreas Kronenberg for their thoughtful reviews and constructive criticism. A. T.

thanks the Conselho Nacional de Desenvolvimento Científico e Tecnológico (CNPq, Brazil) for a Ph.D. fellowship. This work is a contribution to EEC project # CI 1-0320-F-CD "Ductile Shear Zones in the Pan-African Belts from Northeast Brazil and Associated Phanerozoic Sedimentary Basins."

References

Achauer, U., and the KRISP Teleseismic Working Group, New ideas on the Kenya rift based on the inversion of the combined dataset of the 1985 and 1989/90 seismic tomography experiments, *Tectonophysics, 236*, 305-329, 1994.

Beurlen, H., A. F. Da Silva Filho, I. P. Guimarães, and S. B. Brito, Proterozoic C-type eclogites hosting unusual Ti-Fe±Cr±Cu mineralization in northeastern Brazil, *Precambrian Res., 58*, 195-214, 1992.

Bird, P., New finite element techniques for modeling deformation histories of continents with stratified temperature-dependent rheology, *J. Geophys. Res., 94*, 3967-3990, 1989.

Brito Neves, B. B., W. R. Van Schmus, M. Babinski, and T. Sabin, O evento de magmatismo de 1,0 Ga nas faixas móveis ao norte do Cráton do São Francisco, in *Proceedings of the Second Simpósio do Craton do São Francisco*, pp. 243-245, Soc. Bras. de Geol., Rio de Janeiro, 1993.

Buck, W. R., Small-scale convection induced by passive-rifting: The cause for uplift of rift shoulders, *Earth Planet. Sci. Lett., 77*, 362-372, 1986.

Chéry, J., F. Lucazeau, M. Daignières, and J. P. Vilotte, Strain localization in rift zones (case of thermally softened lithosphere): A finite element approach, *Bull. Soc. Géol. Fr., 3*, 437-443, 1989.

Chéry, J., J. P. Vilotte, and M. Daignières, Thermomechanical evolution of a thinned continental lithosphere under compression: Implications for the Pyrenees, *J. Geophys. Res., 96*, 4385-4412, 1991.

Chopra, P. N., and M. S. Paterson, The experimental deformation of dunite, *Tectonophysics, 78*, 453-473, 1981.

Chopra, P. N., and M. S. Paterson, The role of water in the deformation of dunite, *J. Geophys. Res., 89*, 7861-7876, 1984.

Cordell, L., Yu. A. Zorin, and G. R. Keller, The decompensative gravity anomaly and deep structure of the region of the Rio Grande rift, *J. Geophys. Res., 96*, 6557-6568, 1991.

Corsini, M., A. Vauchez, C. J. Archanjo, and E. F. Jardim de Sá, Strain transfer at a continental scale from a transcurrent shear zone to a transpressional fold belt: The Patos-Seridó belt system, (northeastern Brazil), *Geology, 19*, 586-589, 1991.

Davis, P. M., P. Slack, H. A. Dalheim, W. V. Green, R. P. Meyer, U. Achauer, A. Glahn, and M. Granet, Teleseismic tomography of continental rifts, in *Seismic tomography: Theory and practice*, edited by H. M. Iyer and K. Hirahara, Chapman and Hall, New York, pp. 397-439, 1993.

Daudré, B., La localisation de la déformation continentale: Contribution à sa caractérisation numérique. Application à la lithosphère continentale, thèse d'Université, Univ. Montpellier II, Montpellier, France, 1991.

Dunbar, J. A., and D. S. Sawyer, How preexisting weaknesses control the style of continental breakup, *J. Geophys. Res., 94*, 7278-7292, 1989.

England, P., Constraints on extension of continental lithosphere, *J. Geophys. Res., 88*, 1145-1152, 1983.

England, P., and G. Houseman, Role of lithospheric strength heterogeneities in the tectonics of Tibet and neighbouring regions, *Nature, 315*, 297-301, 1985.

England, P., and G. Houseman, Finite strain calculations of continental deformation. 2. Comparison with the India-Asia collision zone, *J. Geophys. Res., 91*, 3664-3676, 1986.

England, P., and G. Houseman, Extension during continental convergence, with applicaton to the Tibetan Plateau, *J. Geophys. Res., 94*, 17561-17579, 1989.

England, P., and D. McKenzie, A thin viscous sheet model for continental deformation, *Geophys. J. R. Astron. Soc., 70*, 295-321, 1982.

Féraud, G., L. L. Figueiredo, M. Corsini, R. Caby, A. Vauchez, and G. Ruffet, Thermo-tectonic evolution of a syn-orogenic lithospheric shear zone through a detailed single grain $^{40}Ar/^{39}Ar$ study: Patos area, Late Proterozoic Brasiliano belt of northeast Brazil, in *Terra Nova Abstr., 5*, 386, 1993.

Houseman, G., and P. England, Crustal thickening versus lateral expulsion in the Indian-Asian collision, *J. Geophys. Res., 98*, 12,233-12,249, 1993.

James, D. E., M. Assumpção, J. A. Snoke, L. C. Ribotta, and R. Kuehnel, Seismic studies of continental lithosphere beneath SE Brazil, *Rev. Bras. de Geofís., in press*, 1995.

KRISP Working Group, Group takes a fresh look at the lithosphere underneath Southern Kenya, *Eos Trans. AGU, 76*, 73, 81-82, 1995.

Leterrier, J., E. Jardim de Sá, J.-M. Bertrand, and C. Pin, Ages U-Pb sur zircon de granitoides brasilianos de la ceinture du Serido (Province Borborema, NE Brésil), *C. R. Acad. Sci. Paris, Ser. Sci. Terre Planetes, 318*, 1505-1511, 1994.

Linch, H. D., and P. Morgan, Finite-elements of continental extension, *Tectonophysics, 174*, 115-135, 1990.

Lowe, C., and G. Ranalli, Density, temperature and rheological models for the southeastern Canadian Cordillera: Implications for its geodynamical evolution, *Can. J. Earth Sci., 30*, 77-93, 1993.

Moreira, J. A. M., W. E. Medeiros, F. A. P. Ling, and C. J. Archanjo, Uma anomalia magnética de caracter regional no Seridó (RN/PB) e discussão de sua origem, *Rev. Bras. de Geofís., 7*, 81, 1989.

Neves, S. P., and A. Vauchez, Magma emplacement and shear zone nucleation and development in northeast Brazil, *J. South Am. Earth Sci., in press*, 1995.

Paterson, M. S., and F. C. Luan, Quartzite rheology under geological conditions, in *Deformation Mechanisms, Rheology and Tectonics*, edited by R. J. Knipe and E. H. Rutter, *Geol. Soc. London Spec. Publ.*, London, *54*, 299-307, 1990.

Peltzer, G., and P. Tapponnier, Formation and evolution of strike-slip faults, rifts, and basins during the India-Asia collision: An experimental approach, *J. Geophys. Res., 93*, 15,085-15,117, 1988.

Prodehl, C., and P. W. Lipman, Crustal structure in the Rocky Mountain region, in *Geophysical Framework of the Continental United States*, edited by L.C. Parkiser and W. D. Mooney, *Mem. Geol. Soc. Am., 1972*, 249-284, 1989.

Sá, J. M., Evolution géodynamique de la Ceinture proterozoique d'Orós, nord-est du Brésil, thèse d'Université, Univ. Nancy I, Nancy, France, 1991.

Sahagian, D. L., and S. M. Holland, On the thermo-mechanical evolution of continental lithosphere, *J. Geophys. Res., 98*, 8261-8274, 1993.

Sibson, R. H., Frictional constraints on thrust, wrench and normal faults, *Nature, 249*, 542-544, 1974.

Thompson, R. N., and S. A. Gibson, Magmatic expression of lithospheric thinning across continental rifts, *Tectonophysics, 233*, 41-68, 1994.

Van Schmus, W. R., B. B. Brito Neves, P. Hackspacker, and M. Babinski, Identification of crustal blocks in northeast Brazil using Sm-Nd and U-Pb geochronology, in *Proceedings of the Second Simpósio do Craton do São Francisco*, pp. 239-242, Soc. Bras. de Geol., Rio de Janeiro, 1993.

Vauchez, A., and G. Barruol, Importance of tectonic heritage in the structure of the Appalachians and the Pyrenees: Insights from shear waves splitting, *Phys. Earth Planet. Inter., in press*, 1995.

Vauchez, A., and M. Egydio-Silva, Termination of a continental-scale strike-slip fault in partially melted crust: The West-Pernambuco shear zone, northeast Brazil, *Geology, 20*, 1007-1010, 1992.

Vauchez, A., and A. Tommasi, Initiation and propagation of shear zone systems in an heterogeneous continental lithosphere, paper presented at International Conference on Structures and Deformation at Different Lithospheric Levels, Univ. Graz, Graz, Austria, 1993.

Vauchez, A., et al., The continental-scale shear zone system of NE Brazil, an example of Panafrican intraplate tectonics, *Comunicaciones, 42*, 233-237, 1991.

Vauchez, A., A. Tommasi, and M. Egydio-Silva, Self-indentation of continental lithosphere, *Geology, 22*, 967-970, 1994.

Vauchez, A., S. Pacheco-Neves, R. Caby, M. Corsini, M. Egydio-Silva, M. Arthaud, and V. Amaro, The Borborema shear zone system, *J. South Am. Earth Sci., in press*, 1995.

Vilotte, J.-P., M. Daignières, and R. Mandariaga, Numerical modeling of intraplate deformation: Simple mechanical models of continental collision, *J. Geophys. Res., 87*, 10,709-10,728, 1982.

Vilotte, J.-P., R. Mandariaga, M. Daignières, and O. Zienkiewicz, The role of a heterogeneous inclusion during continental collision, *Phys. Earth Planet. Inter., 36*, 236-259, 1984.

Vilotte, J.-P., R. Mandariaga, M. Daignières, and O. Zienkiewicz, Numerical study of continental collision: Influence of buoyancy forces and an initial stiff inclusion, *Geophys. J. R. Astron. Soc., 84*, 279-310, 1986.

Vitorello, I., V. M. Hanza, and H.N. Pollack, Terrestrial heat flow in the Brazilian highlands, *J. Geophys. Res., 85*, 3778-3788, 1980.

Wdowinski, S., and Y. Bock, The evolution of deformation an topography of high elevated plateaus, 1, Model, numerical analysis, and general results, *J. Geophys.Res., 99*, 7103-7119, 1994.

Wilks, K. R., and N. L. Carter, Rheology of some continental lower crust rocks, *Tectonophysics, 182,* 57-77, 1990.

Zorin, Yu. A., V. M. Khozevnikov, M. R. Novoselova, and E. K. Turutanov, Thickness of the lithosphere beneath the Baikal rift and adjacent regions, *Tectonophysics, 168*, 327-337, 1989.

B.Daudré, IREMIA, Université de la Réunion, F-974 St.Denis, La Réunion, France. (email: daudre@univ-reunion.fr)

A.Tommasi and A.Vauchez, Laboratoire de Tectonophysique, USTL, Place Eugène Bataillon, F-34095 Montpellier cedex 5, France. (email: deia@dstu.univ-montp2.fr; vauchez@dstu.univ-montp2.fr;)

(Received August 18, 1994; revised June 21,1995;
accepted June 27, 1995.)